PERGAMON

Applied Thermal Engineering 20 (2000) 671–685

APPLIED THERMAL ENGINEERING

www.elsevier.com/locate/apthermeng

Heat transfer and pressure drop in ice-water slurries

B.D. Knodel[a], D.M. France[b,*], U.S. Choi[c], M.W. Wambsganss[c]

[a]*Ethicon Endo-Surgery, Inc., Cincinnati, OH 45242-2839, USA*
[b]*Department of Mechanical Engineering (m/c 251), University of Illinois at Chicago, 842 W. Taylor Street, Chicago, IL 60607-7022, USA*
[c]*Energy Technology Division, Argonne National Laboratory, Argonne, IL 60439, USA*

Abstract

Heat transfer and pressure drop were experimentally investigated for ice-water slurries flowing turbulently in a 24.0 mm internal diameter, 4.596 m long, horizontal, stainless steel tube. The slurry velocity of the experiments was varied from 2.8 to 5.0 m/s which encompassed the range of applicability to ice-water slurry-based district cooling systems. The previously reported phenomenon of flow relaminarization in ice-water slurries was observed in the current experiments. A reduction in frictional pressure drop associated with the flow relaminarization was measured as the ice fraction increased. An ice fraction of 4% marked a division in the rate of reduction, and a pressure-drop correlation equation was developed for ice fractions above 4%. Heat transfer coefficients were determined over the velocity range of the experiments. Consistent with the flow relaminarization, the heat transfer coefficient decreased with increasing ice fraction. A correlation equation was also developed for heat transfer coefficients at ice fractions above 4%.

Keywords: Ice; Slurry; Heat transfer; Pressure drop; District cooling

1. Introduction

Historically, district cooling systems have been most utilized in new construction of universities, military bases, multi-building laboratories, etc. where a high density of buildings is under single administrative control. The number of utility companies that service commercial cooling needs with district systems has been small. However, with the changes in acceptable

* Corresponding author. Fax: +1-312-413-0447.

1359-4311/00/$ - see front matter
PII: S1359-4311(99)00046-0

refrigerants for large air-conditioning systems, there has been interest in utility-operated district cooling systems for commercial buildings in high-density metropolitan areas. Salient examples are the several district-cooling plants that operate or are under construction in the downtown area of Chicago, IL, USA. All of these conventional district cooling systems deliver chilled water to buildings in close proximity to the plants with the cooling loads limited by both the installed plant equipment and the size of the delivery piping.

The emergence of ice-water slurries for use in district cooling systems may be the most significant technical development since the birth of the industry. The large energy capacity of ice-water slurries, when compared to conventional chilled-water systems, can potentially reduce the distribution flow rate by over 80% in existing plants while maintaining the same cooling load and pumping power, or it can increase the cooling capacity up to 600% at the same flow rate and pumping power [1,2]. In new district cooling plants, lower flow rates result in pipe diameter reductions of up to 65% and proportionally smaller pumps. These factors combine to lower both the capital and operating costs of district cooling systems, and for existing chilled water systems, ice-water slurries can significantly increase the cooling capacity without requiring increases in distribution pipe size or system flow rates. These potential changes are based on the ability to create ice-water slurries with relatively high ice fractions (percent by mass of ice in the ice-water slurry) of up to 30%. However, even at a relatively low ice fraction of 5%, Choi et al. [2] showed that the cooling capacity of an existing district cooling system would be increased by a factor of two at the same pumping power. This increase, of 100% in cooling capacity by introducing an ice-water slurry with an ice fraction as low as 5% into an existing district cooling system, supports the contentions of the significance of this technology to district cooling.

Use of ice-water slurries in district cooling systems requires knowledge of both the fluid mechanics and heat transfer characteristics of the slurry. There have been a few publications on the subject of pressure drop and flow characteristics of ice-water slurries, e.g. [3,4], but there are no known publications on heat transfer to such slurries. It was the primary objective of this investigation to study the heat transfer to ice-water slurries flowing in horizontal pipes for application to district cooling systems. An experimental approach was taken in which an ice-water slurry was generated and pumped in a closed system Heat was added at controlled rates producing a relatively slow transient (quasi-steady) situation as the ice melted and data were collected.

2. Experimental apparatus

The ice-water-slurry experimental facility at Argonne National Laboratory was redesigned for the present study and is shown schematically in Fig. 1. The facility had the capability of generating ice particles or accepting ice particles introduced in a batch process. In either case, the ice particles were slurried with water and introduced into the system piping. The ice-water slurry thus formed was pumped in a continuous piping loop through the test section. During heat transfer tests, heat was applied to the test section melting the ice at prescribed rates. Temperatures, pressures, power, and flow were measured in the facility at locations indicated in Fig. 1.

2.1. Ice generation system

The ice generation system in the experimental facility is based on a patented, high-efficiency, direct-freeze process [5,6]. In this process, water and refrigerant are mixed as liquids in a direct-contact heat exchanger causing a portion of the water to freeze as the refrigerant vaporizes. This direct-freeze ice generation system efficiently produced ice crystals with diameters in the range of 2–3 mm for the present study. It took 10–20 min to produce enough ice for each of the various experiments performed. Generation of ice as part of the experimental facility was a very convenient feature as opposed to generating it externally and transporting it to the facility while minimizing heat gain and melting.

2.2. Ice-water slurry distribution system

Once ice crystals were collected in the ice-water pressure vessel shown in Fig. 1, it was necessary to form a slurry with water and to introduce it into the experimental facility piping. This task could be difficult because the ice crystals adhere to one another and to the vessel walls. In the present study, an ice-water slurry was successfully formed by first collecting the ice crystals on water at the bottom of the pressure vessel. As the generator continued to produce ice, the concentration of the crystals on the water increased. At desired concentrations, an ice-water slurry was drawn off the surface of the water and introduced into the facility piping at the slurry-pump suction.

The slurry pump used in the experimental facility was a positive displacement screw type design. It was driven by a variable-speed direct-drive motor, and it was capable of delivering ice-water slurry flow rates from 0.30 to 3.8 l/s.

2.3. Test section

The test section fabricated for the present study is also shown in Fig. 1. It was constructed

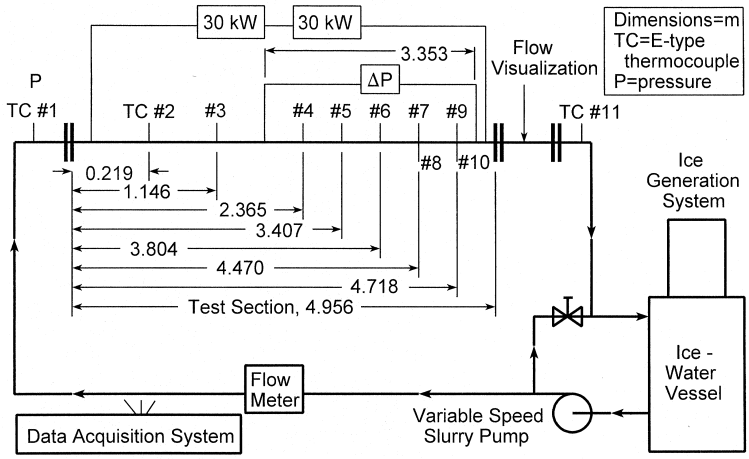

Fig. 1. Experimental facility.

from a thin-wall, Type 304 stainless steel tube with an inside diameter of 24.0 mm and a 0.71 mm wall thickness. Heat was supplied, by two 30 kW power supplies in series, to the slurry flowing in the tube by passing direct electric current through the tube wall. The electrical energy input was determined by measuring the voltage drop across the heated portion of the test section and its current (using a calibrated shunt resistor). All signals from the power supply, test section instruments and flow meter were read on a computer controlled data acquisition system (DAS).

Type E stainless-steel-sheathed thermocouples with a diameter of 3.2 mm were placed in the inlet and outlet flow streams. Type E wire thermocouples were placed on the outer surface of the tube wall. The axial locations of the wall thermocouples are given in Fig. 1. At locations of 4.470 and 4.718 m, thermocouples were placed on both the top and bottom of the tube as a consistency check. An end-to-end calibration, performed on the test section thermocouples in place through the DAS, registered an accuracy of $\pm 0.2^{\circ}C$. This portion of the test section was thermally well insulated from the environment, and it was followed by a glass section that provided flow visualization when ice crystals were present. Heat loss tests were performed to quantify the small heat loss from the test section.

2.4. Flow and pressure measurements

Flow measurement of the ice-water slurry was made in the unheated pipe upstream of the test section entrance. The flow meter shown in Fig. 1 was a paddle-wheel type that allowed the ice-water slurry to move through the relatively large spaces between the blades. The flow meter accuracy was $\pm 5\%$ of the reading.

Pressure drop of the ice-water slurry was measured across the downstream portion of the test section using an electronic differential pressure transducer with an accuracy of better than ± 0.3 kPa.

3. Experimental procedure

Each heat transfer test was run as a slow (quasi-steady) transient in which the ice fraction decreased as heat was applied to the test section. Initially, flow was established in the system with the slurry pump at a prescribed test section velocity in the range of 2.8–5.0 m/s. The ice generation system was then started. After an ice-water slurry was produced and introduced into the system at an ice fraction of approximately 11%, the generation system was stopped and isolated from the system. Electric power was then applied to the test section while the ice-water slurry continued to be pumped in a closed loop through the test section. The ice melted gradually (over several minutes) due to heat input from the test section, the surroundings, and the pump. A data scan consisted of a set of readings of all of the instruments: flow meter, pressure transducer, thermocouples, and power. Multiple scans of data were taken by the DAS, averaged, and stored as one data point for the test. Data points were stored at 1–5 s intervals depending on the duration of the test. The signal averaging process reduced electronic noise to a minimum, and typically each recorded data point was an average of 20 scans. Data points were recorded from the start of heating, with the initial ice fraction of the order of 11%,

to the time when all of the ice had melted and the water temperature began to rise above 0°C. This procedure produced data from the initial 11% ice fraction to zero in a single test (and at a single flow rate). Tests of this type were conducted over a range of flow rates.

During each test, data continued to be accumulated by the DAS after all of the ice had melted. When the system contained water in the liquid state in the 0–2°C temperature range, the data were used to determine the ice fraction during the test by first determining the total heat input rate. Measurements of the fluid temperature in the test section identified the time at which zero ice fraction was achieved. The total rate of energy input, Q, was determined from the ensuing transient in the liquid from the energy storage

$$Q = mC_v \frac{dT}{dt} \tag{1}$$

where Q (W) is the total heat transfer rate, m (kg/s) is the flow rate of liquid, C_v (kJ/kg K) is the liquid specific heat, T (°C) is the liquid temperature, and t (s) is time. Once Q was determined from the liquid part of the transient, the ice fraction was calculated throughout the melting portion of the transient assuming that the rate of energy input had been constant for the entire time. In addition to the test section power input, this procedure accounted for the parasitic effects on ice melting rate of environmental energy input and pump energy input.

4. Data analysis

4.1. Pressure drop analysis

During each test, the Darcy friction factor was determined experimentally as a function of ice fraction from the pressure drop and flow rate measurements. A hydrodynamic entrance length of over 50 diameters in the test section preceded the upstream pressure tap as shown in Fig. 1. This arrangement avoided entrance effects in the region of the test section where pressure measurements were made. Pressure drops were measured in all ice-water-slurry tests as well as in tests that employed single-phase water in the liquid state. Data from the all-liquid tests (circular symbols) are seen in Fig. 2 to be in good agreement with a standard smooth-tube turbulent friction factor equation,

$$f = 0.184 Re_D^{-0.2} \tag{2}$$

The liquid friction factor results were used subsequently as a reference of comparison for the ice-water slurry pressure drop data.

4.2. Heat transfer analysis

Heat transfer tests were also performed with only liquid flowing in the test section. The heat transfer coefficients were determined from the measured heat input, test section wall temperatures, and liquid temperatures. These heat transfer coefficients (square symbols) are seen in Fig. 2 to compare favorably with the Petukhov [7] correlation equation

$$Nu_D = \frac{(f/8)Re_D Pr}{K_1 + K_2(f/8)^{1/2}(Pr^{2/3} - 1)} \tag{3}$$

where

$$K_1 = 1 + 3.4f \tag{4}$$

$$K_2 = 11.7 + 1.8Pr^{-1/3} \tag{5}$$

and the friction factor, f, in Eqs. (3) and (4) is given by

$$f = \left(1.82 \log_{10} Re_D - 1.64\right)^{-2} \tag{6}$$

In Eq. (3), Nu_D is the Nusselt number based on the inside tube diameter, D (m); Re_D is the Reynolds number based on D, and Pr is the Prandtl number.

Both the heat transfer and pressure drop comparisons for the liquid tests provided overall verification of the test facility procedures, instrumentation, and data acquisition/reduction methods. These same techniques were used with the subsequent ice-water-slurry tests.

During each ice-water-slurry test, local heat transfer coefficients were determined along the test section at each location of a tube wall thermocouple according to the standard definition, $h = q/(T_{w,i} - T_b)$. (The heat transfer coefficient is designated by h (W/m^2 K); q is the heat flux (W/m^2), and the subscripts 'w,i' and 'b' refer to the inside tube wall and bulk fluid, respectively.) In the case of the ice-water slurry, the bulk fluid temperature T_b was constant at 0°C. (In the case of the liquid tests discussed previously, T_b was determined from a heat balance along the test section.) The heat flux was determined from the measured electrical power input, and the wall temperature $T_{w,o}$ was measured on the outside of the tube. The inside tube wall temperature $T_{w,i}$ was calculated from a radial conduction model including the effect of the heat generation in the wall. The result is

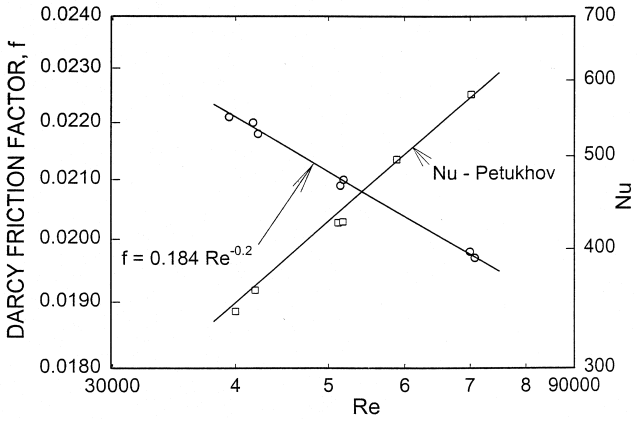

Fig. 2. Liquid test verification.

$$T_{w,i} = T_{w,o} - \left[\frac{Q}{2\pi(r_o^2 - r_i^2)Lk_w}\right]\left[r_o^2 \ln(r_o/r_i) + 0.5(r_i^2 - r_o^2)\right] \quad (7)$$

where r_i and r_o are the tube inside and outside radii, respectively. The heated test section length is L (m), and k_w (W/m K) is the thermal conductivity of the tube material.

5. Results

5.1. Ice-water-slurry pressure drop

Pressure drop results for a typical ice-water-slurry test are shown in terms of the Darcy friction factor in Fig. 3. In the test shown, the ice fraction started above 10%, and the solid symbols represent the measured friction factors during the test as the ice fraction reduced to zero. Also shown in Fig. 3 are liquid friction factors calculated from Eq. (2). There was some Reynolds number variation during the test as seen in these liquid friction factors, but each calculation was made at the local Reynolds number, and the initial Reynolds number for the test was 58,000 as given in the figure. The smooth-tube friction factor of Eq. (2) shows good agreement with the data as ice fraction goes to zero.

A very interesting result is shown in Fig. 3 where it is observed that the ice-water slurry friction factor decreases with increased ice fraction in a nonlinear manner. This dependence is opposite to what is normally found with particles suspended in a fluid where friction is increased with particle concentration. At low ice fractions under about 2%, it is observed in Fig. 3 that there is little difference between the friction factors of the ice-water slurry and liquid water. Both friction factors are approximately constant in that ice fraction range. A steep decrease occurs in the ice-water-slurry friction factor between 2 and 4% ice fraction, and

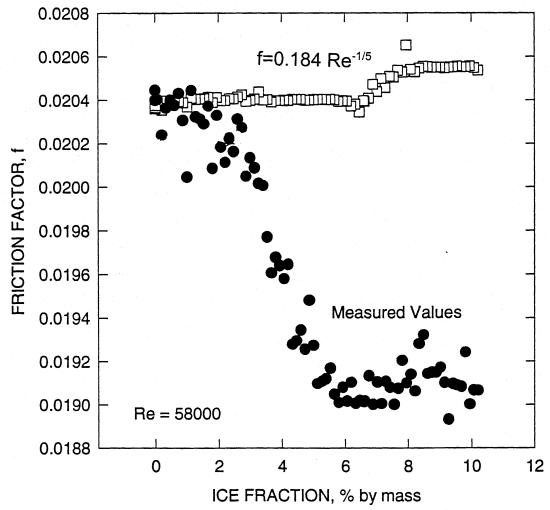

Fig. 3. Typical ice-water slurry friction test data.

above 4% the slurry friction factor becomes approximately constant again. This behavior of decreasing friction factor with increased ice fraction was observed previously by Knodel and France [3] with similar size ice crystals in an ice-water slurry. In contrast, this phenomenon has not been observed in ice-water slurries with small (less than 1 mm diameter) ice crystals (Matthys [8]).

Although Matthys [8] did not observe the pressure drop reduction phenomenon with ice particles of less than 1 mm diameter, Liu et al. [9] clearly observed the phenomenon with cross-linked, high-density-polyethylene (X-HDPE) particles with diameters of 1.3 mm. A critical upper limit on particle loading was also found, in these HDPE-water slurries, above which the pressure drop reduction phenomenon disappeared; the threshold was about 30%. Sharp increases in pressure drop were observed above the critical upper limit particle loading. However, it was pointed out [9] that this critical upper-limit on particle loading is sufficiently high as to retain the pressure drop reduction benefits for many applications. The maximum ice fractions of the present study were approximately 11%, and a critical upper limit was not observed at these loadings.

The results of the present study agree qualitatively with those of Liu et al. [9] in that both exhibited the pressure drop reduction phenomenon. However, the maximum reduction was larger for the ice slurries used in this study (about 5%) than for the HDPE slurries (about 2%). The physical phenomenon resulting in the drag reduction is the reduced turbulence level of the fluid as a consequence of particle-fluid interaction. This phenomenon has been characterized as a relaminarization process by analogy to turbulence levels in single phase flow.

In contrast to the ice-water slurry used in the present investigation, binary-solution ice-water slurries typically consist of much smaller diameter ice crystals. Reports by Graham et al. [10], Gupta and Fraser [11], and Larkin and Young [12] were all based on a slurry that was generated with a mixture of water and ethylene glycol (used as a freezing-point depressant in the ice generation process). Ice particle diameters in these slurries were in the range of 0.1–0.25 mm. It was found that the slurry pressure drop at ice fractions up to about 30% was essentially the same as that of a solution of water and glycol of the same concentration, approximately 6% ethylene glycol. (This 30% ice-fraction threshold was velocity dependent.) At higher ice fractions above approximately 30%, the two pressure drops diverged. The very small size of the ice crystals in the binary-solution ice-water slurry is believed to be inefficient in decreasing fluid turbulence and thus produces no drag reduction in the range where larger ice crystals (2–3 mm in this study) show a substantial reduction.

The ice-water-slurry friction factor data were normalized by the liquid predictions from Eq. (2). The resulting friction factor ratio is shown in Fig. 4 for the same test that is shown in Fig. 3. The ratio has a value of unity at zero ice fraction and asymptotes to another constant value at ice fractions above approximately 4%.

Ice fraction asymptotic friction factor results above 4% are shown in Fig. 5 over the Reynolds number range of the data. The data are plotted for constant ice fractions of 4, 6, 8, and 10%. (Ice fractions below the 4% value fall within the transition zone where the slurry friction factor decreases with increased ice fraction.) The solid horizontal line in Fig. 5 represents the all-liquid friction factor ratio of unity. The broken line represents the mean value of the data which is relatively constant at 5.4% friction factor reduction.

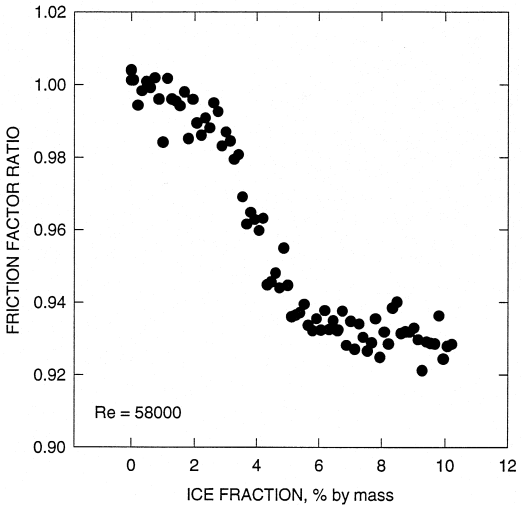

Fig. 4. Ice-water slurry friction relative to liquid.

5.2. Ice-water-slurry heat transfer

Typical ice-water-slurry heat transfer results are presented in Figs. 6 and 7 at approximately the same Reynolds number and two different test section heat fluxes. The Nusselt number at zero ice fraction is well predicted by the Petukhov [7] correlation as seen in both figures. A decrease in Nusselt number with increased ice fraction is observed up to a value of approximately 4% ice fraction. At higher ice fractions, the Nusselt number is relatively constant.

The Petukhov [7] correlation was used to normalize the heat transfer data producing a

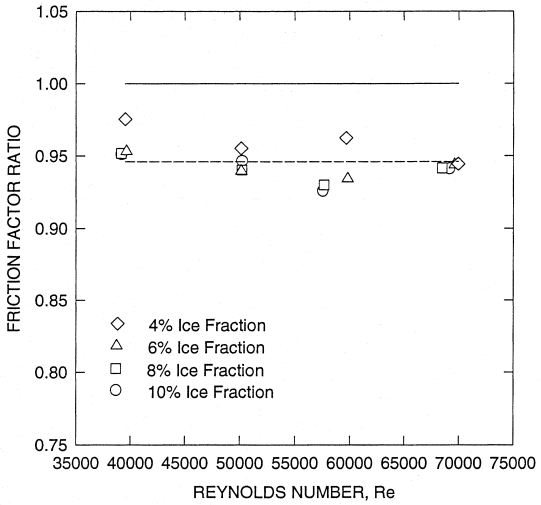

Fig. 5. Ice-water slurry friction above 4% ice fraction.

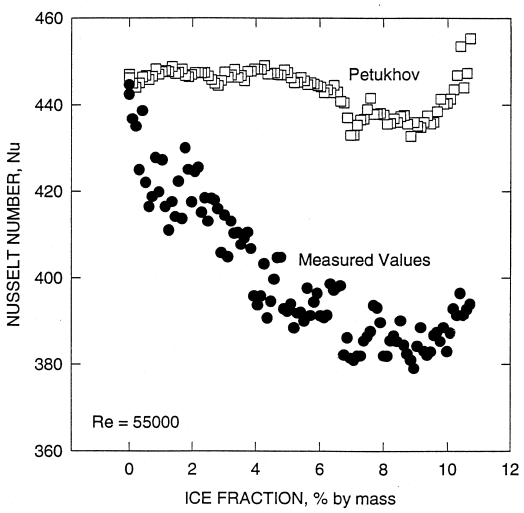

Fig. 6. Typical ice-water slurry heat transfer test data at 15 kW/m^2.

Nusselt number ratio, i.e., the ice-water-slurry Nusselt number relative to single-phase water. Results are shown in Figs. 8 and 9 at constant Reynolds number and the same two heat fluxes of Figs. 6 and 7, respectively. The Nusselt number ratio decreases from unity at zero ice fraction to a relatively constant value at ice fractions greater than 4%. (The 4% cutoff is clearer when the Nusselt number ratios are plotted.) Taking all of the heat transfer data together at ice fractions greater than 4%, the Nusselt number ratio was found to be 11.5% lower than the equivalent liquid value as shown in Fig. 10. (Fig. 10 parameters are similar to those explained for Fig. 5.)

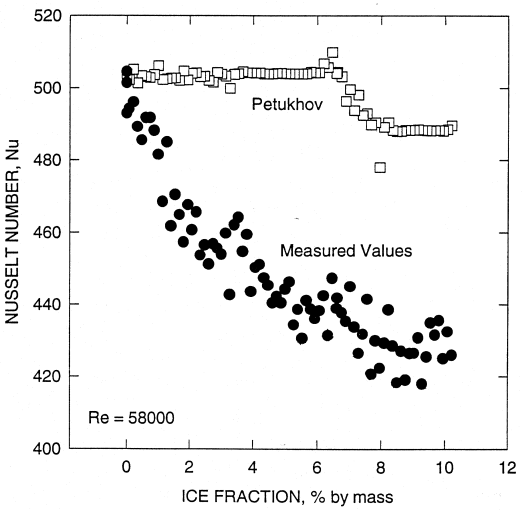

Fig. 7. Typical ice-water slurry heat transfer test data at 40 kW/m^2.

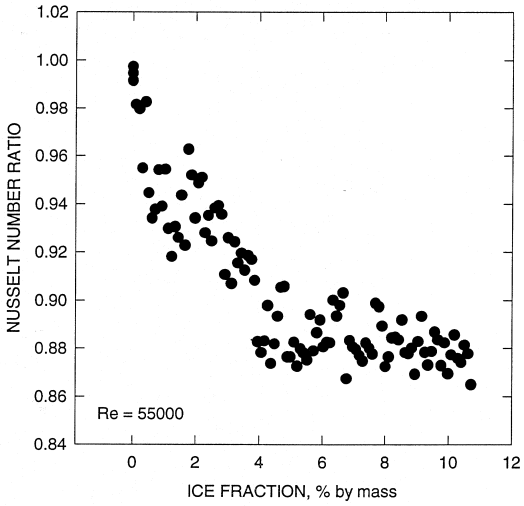

Fig. 8. Slurry heat transfer relative to liquid at 15 kW/m^2.

6. Discussion

6.1. Pressure drop characteristics

After a series of experiments, the friction reduction behavior of ice-water slurries was reported first by Knodel [13], and again by Knodel [14] and Knodel and France [3,4]. The results were obtained in larger diameter channels (48 and 100 mm), compared to the 24 mm tube of this study, with similar size ice crystals and ice fractions to the present study. The previous results showed a reduction in friction factor as ice fraction increased to 8% followed

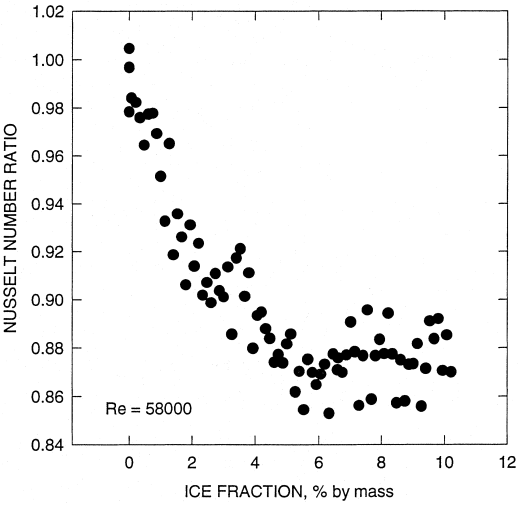

Fig. 9. Slurry heat transfer relative to liquid at 40 kW/m^2.

by a constant friction factor at higher ice fractions. These results differ from the current study in the transition ice fraction at which friction reduction ceases, 4% in the current study versus 8% in the larger tubes. However, the same phenomenon of relaminarization of the flow was found to occur in all tubes at ice fractions greater than the transition and is consistent with the friction reduction. In all cases, the flows were turbulent at zero ice fraction. As ice fraction increased, turbulent eddies were observed to decrease until, at ice fractions above the transition, the flows appeared laminar to the observer with no noticeable turbulence. (The ice crystals provided inherent flow visualization.)

Another difference was observed between the large-tube data and the current data. The functional relationship developed for friction factor (Knodel and France [4]), at ice fractions greater than the transition (8%) in the large tubes, did not predict the current data well at ice fractions above the transition of 4%. It is believed that the small tube diameter of this study was the cause of this prediction difference as well as the change in transition ice fraction. There was an audible indication of more interaction between the 2–3 mm diameter ice crystals and the current 24 mm diameter tube than in the previous studies with 48 and 100 mm diameter tubes. Thus, using the same size ice particles in all tubes, the indication was that more particle-wall interaction occurred in the small diameter tube of this study. As a result, it appears that the turbulence suppressing mechanism of the particles was partially counteracted by additional wall friction caused by the particles. The net result was the general characteristics of the friction reduction were the same for the small and large tubes, but the magnitudes and transition ice fractions were different.

Friction reduction behavior in solid–liquid mixtures has been observed by other investigators. Thomas [15–17] measured friction reduction for laminar and turbulent flows of spherical-shaped thoria, kaolin, and titania particles. Stepanoff [18] investigated friction reduction behavior that occurs in pipeline transport of coal slurries. Similarly, Durand [19] observed this behavior in turbulent flows with sand-water and clay-water slurries. The friction

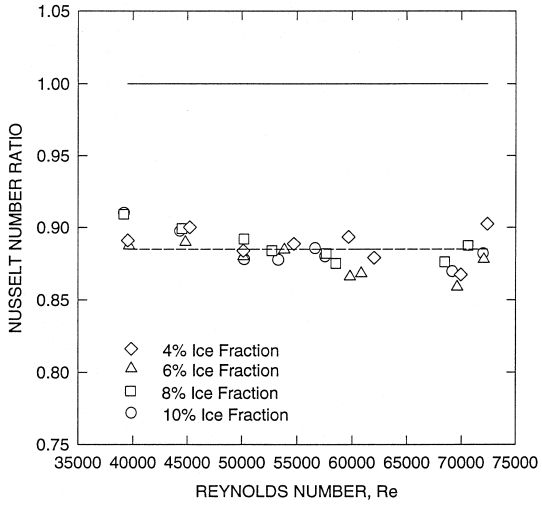

Fig. 10. Ice-water slurry heat transfer above 4% ice fraction.

reduction behavior measured by these investigators has been associated with two primary phenomena. The first is a dampening of turbulence in the core of the flow resulting in a transition from turbulent flow toward a laminar plug flow. (This phenomenon was observed in the ice-water-slurry tests.) The second phenomenon, which was the basis of the friction factor correlation of Knodel and France [4], is the formation of an all-liquid layer at the pipe wall, i.e., a liquid film.

It appears that the reduced pipe diameter of this study, relative to the ice crystal size, impaired the friction reduction behavior of the ice-water slurry. Although the slurry demonstrated a flow transition from turbulent toward laminar plug, its ability to form an all-liquid film at the tube wall appears to have been compromised. The few ice crystals required to fill the cross section of the pipe appear to have restricted the liquid film mechanism. The audible ice-crystal to wall interaction noted only in the small pipes of the current study supports that condition.

6.2. Correlation of pressure drop

The results of Fig. 5, and all of the supporting data in the range of ice fractions from 4 to 11% and Reynolds numbers from 3.8×10^4 to 7.4×10^4 in the 24 mm diameter pipe, imply that a constant multiplier of 0.946 can be applied to the all-liquid friction factor correlation of Eq. (2) to predict the friction factor for ice-water slurries in this small tube at ice fractions above 4% ice by mass. Mathematically, one can write

$$\frac{f_{\text{ice-water slurry}}}{0.184 Re_{\text{D}}^{-0.2}} = 0.946 \tag{8}$$

6.3. Heat transfer characteristics

The same phenomenon of flow relaminarization that is considered the cause of the friction reduction in ice-water slurries is also attributed with the decrease in heat transfer rates. The flow moving from a turbulent condition toward laminar reduces the heat transfer coefficient. In the case of friction reduction, the result is positive. However, in the case of heat transfer coefficient, it can be viewed as either positive or negative depending on the application. In the case of an ice-water slurry moving through a heat exchanger, reduced heat transfer coefficient of the slurry is undesirable because it leads to larger heat exchangers. However, in the process of transporting an ice-water slurry through a pipe, heat transfer to the surroundings is to be minimized, and the reduction in heat transfer coefficient is then viewed as a positive effect.

As discussed in Ref. [2], district cooling systems that employ ice-water slurries need not pump the slurry through heat exchangers in order to reap benefits from the slurry. However, pumping to remote sites from the generating site is necessary to obtain full benefit from the slurry. Thus, if ice-water-slurry transport, not heat exchanger use, is the important factor in a district cooling system, then the reduced heat transfer coefficient of the slurry compared with that of liquid water is a positive condition for that application.

8.4. Correlation of heat transfer

Referring to Fig. 10 for the same parameters as Eq. (8), the Nusselt number for ice-water slurries in small-diameter tubes can be related to single-phase liquid flow. A multiplier of 0.885 is obtained relating the ice-water-slurry Nusselt number to the Petukhov [7] liquid correlation, or

$$\frac{Nu_{\text{ice-water slurry}}}{Nu_{\text{Petukhov}}} = 0.885 \tag{9}$$

7. Conclusions

Ice-water slurries have been shown to produce reductions in pressure drop in the relatively small-diameter tube of this study. The transition ice fraction differed from previous results in larger-diameter tubes, but the same trends were observed.

Result of this study represent the first heat transfer coefficient measurements reported in ice-water slurries. Heat transfer coefficient reduction was also found with the ice-water slurries compared to liquid water flowing at the same Reynolds number. Both reductions in friction factor and heat transfer coefficient occurred as the flow transitioned from turbulent to laminar plug as the ice fraction increased. The maximum reduction in both the friction factor and Nusselt number values was coincident with the flow reaching the laminar plug type structure. At ice fractions above the transition ice fraction, further reductions in friction factor and Nusselt number were not observed.

The friction factor, in small-diameter pipes for ice-water slurries as in this study, has been correlated as a constant multiplier to the turbulent liquid friction factor for smooth tubes of Eq. (2). The Nusselt number for these ice-water slurries has been correlated as a constant multiplier to the Petukhov heat transfer correlation for a single-phase fluid flowing turbulently in a smooth pipe, Eq. (3).

Acknowledgements

The experiments of this study were performed at Argonne National Laboratory with the support of the US Department of Energy, Community Research and Development Branch, Utility Systems Division, Energy Efficiency and Renewable Energy Programs, Washington, DC under Contract W-31-109-Eng-38.

References

[1] P. Metz, P. Margen, The feasibility and economics of slush ice district cooling systems, ASHRAE Transactions 932 (2) (1987) 1672–1686.

[2] U.S. Choi, D.M. France, B.D. Knodel, Impact of advanced fluids on costs of district cooling systems, in:

Proceedings of the 83rd Annual Conference of the International District Heating and Cooling Association, Danvers, MA, 1992, pp. 344–359.
[3] B.D. Knodel, D.M. France, Pressure drop in ice-water slurries for thermal storage applications, Experimental Heat Transfer 1 (1987) 265–275.
[4] B.D. Knodel, D.M. France, Ice-water slurry flow in a circular pipe, Intl. Communications in Heat and Mass Transfer 15 (1988) 239–245.
[5] B.D. Knodel, et al., Apparatus and method for cold aqueous liquid and/or ice production, storage and use for cooling and refrigeration, US Patent No. 4,596,120, 1986.
[6] B.D. Knodel, et al., Apparatus and method of ice production by direct refrigerant contact with aqueous liquid, US Patent No. 4,754,610, 1988.
[7] B.S. Petukhov, Heat transfer and friction in turbulent pipe flow with variable physical properties, in: Advances in Heat Transfer, vol. 6, Academic Press, New York, 1970, pp. 503–564.
[8] E.F. Matthys, An experimental study of convective heat transfer, friction, and rheology for non-Newtonian fluids: polymer solutions, suspensions of fibers, and suspensions of particulates, Ph.D. thesis, California Institute of Technology, 1985.
[9] K.V. Liu, U.S. Choi, K.E. Kasza, Measurements of pressure drop and heat transfer in turbulent pipe flows of particulate slurries, Argonne National Laboratory Report, ANL-88-15, Argonne, IL, 1988.
[10] T. Graham, T. Tokunaga, V. Goldstein, Application of crystal ice generation in district heating and cooling, in: Proceedings of the 80th Annual Conference of the IDHCA, Virginia Beach, VA, 1989.
[11] R.P. Gupta, C.A. Fraser, Effect of a new friction reducing additive on Sunwell ice slurry characteristics, National Research Council of Canada, Institute of Mechanical Engineering, Low Temperature Laboratory, TR-LT-023, NRC No. 32123, 1990.
[12] B. Larkin, J.C. Young, Influences of ice slurry characteristics on hydraulic behavior, in: Proceedings of the 80th Annual Conference of the IDHCA, Virginia Beach, VA, 1989.
[13] B.D. Knodel, Performance of an ice-water slurry based district cooling system, in: Proceedings of 78th Annual Conference of the IDHCA, Baltimore, MD, 1987.
[14] B.D. Knodel, Phase II — direct freeze ice slurry district cooling, in: Proceedings of the 80th Annual Conference of the IDHCA, Virginia Beach, VA, 1989.
[15] D.G. Thomas, Progress in Int'l Research in Thermodynamics and Transport Properties, ASME, 1962, pp. 704–717.
[16] D.G Thomas, A.I.Ch.E. Journal 8 (3) (1962) 373–378.
[17] D.G Thomas, A.I.Ch.E. Journal 9 (3) (1963) 310–316.
[18] A.J. Stepanoff, Pumping solid–liquid mixtures, Mechanical Engineering (1964) 29.
[19] R. Durand, Basic relationships of the transportation of solids in pipes, in: Proceedings of Minnesota Hydraulics Convention, 1953, pp. 89–103.